PAPER • OPEN ACCESS

A Differential Time-of-Arrival Localization Method for Underwater Moving Platforms Based on Time Reference Synchronization and Motion Compensation

To cite this article: Xiaoyue Shao *et al* 2026 *J. Phys.: Conf. Ser.* **3178** 012054

A Differential Time-of-Arrival Localization Method for Underwater Moving Platforms Based on Time Reference Synchronization and Motion Compensation

Xiaoyue SHAO[1], Chuanqi ZHU[1*], Liang AN[1]

[1] Key Laboratory of Underwater Acoustic Signal Processing, Southeast University, Ministry of Education, Nanjing 210096, China
Email: chuanqizhu@seu.edu.cn

Abstract. Accurate localization is essential for underwater acoustic networks, but clock offsets among nodes and the motion of mobile platforms degrade traditional time-of-arrival (TOA) methods. High-precision time references, such as atomic clocks, can reduce synchronization errors but incur high cost and power consumption and cannot correct motion-induced propagation-time variations. This paper proposes a lightweight differential TOA (dTOA) localization framework based on time-reference synchronization and motion compensation. Leveraging the broadcast nature of underwater acoustic communications, each fixed beacon sequentially transmits acoustic signals, while the others listen and record reception timestamps. These inter-beacon listening observations establish and maintain a unified time reference without external clocks. For the moving receiver, a motion-compensation model projects measured TOAs onto the unified reference epoch within each localization cycle to remove displacement-induced timing bias. Based on synchronized references and motion-compensated TOAs, we derive a novel differential TOA estimator that directly cancels residual clock biases between the mobile node and the beacon network. Unlike previous approaches requiring absolute time or spatial references, the proposed method simultaneously resolves time asynchrony and motion-related TOA distortion. Simulation and sea-trial results show RRMSE reductions of up to 90% and over 93%, demonstrating the method's robustness and its suitability for energy- and cost-constrained AUV deployments.

1. Introduction

Underwater acoustic localization plays a crucial role in marine monitoring, target tracking, and underwater vehicle navigation[1,2]. In recent years, with the development of underwater acoustic communication networks, accurate and reliable localization has become an essential enabler for a variety of underwater applications[3,4]. However, unlike radio-based localization in terrestrial environments, underwater positioning faces unique challenges due to the slow propagation speed of sound, the time-varying nature of the underwater medium, and the difficulty of achieving precise clock synchronization among nodes[5–7].

Traditional time-of-arrival (TOA) localization methods rely on accurate transmission and reception timestamps between fixed beacons and mobile nodes[8–10]. In practice, however, each beacon maintains its own internal clock, which introduces inevitable time offsets that cause ranging errors[11–13]. Moreover, for autonomous underwater vehicles (AUVs) that move continuously during signal transmission and reception, the propagation path and corresponding travel time vary dynamically, further increasing localization errors[14,15]. Therefore, achieving both temporal synchronization and motion compensation is essential to improving positioning accuracy in underwater networks[16,17].

To address these issues, this paper proposes an underwater localization approach that integrates clock synchronization among fixed nodes and motion-compensated differential time-of-arrival (dTOA) localization for the mobile node. In the proposed framework, three fixed beacons alternately transmit acoustic signals, and by recording the corresponding reception times, an inter-node synchronization model is constructed. This allows all beacons to be synchronized to a common reference without relying on an external time source. Subsequently, when the AUV receives localization signals from the synchronized beacons, a motion compensation model is applied to correct the propagation-time deviations caused by the vehicle's continuous movement. Finally, a differential TOA formulation is adopted to eliminate residual clock biases between the mobile node and the fixed beacon network.

The proposed method has been validated through both simulation and real sea trial experiments. The simulation results demonstrate the effectiveness of synchronization and motion compensation in reducing time-based errors, while the sea trial results verify the method's applicability under real ocean conditions. Compared with conventional TOA localization, the proposed synchronization and dTOA-based method achieves higher positioning stability and robustness in asynchronous and dynamic underwater environments.

The main contributions of this paper are:

- A beacon synchronization scheme eliminating inter-node clock offsets.
- A motion-compensation formula for continuously moving AUVs.
- A differential TOA formulation that removes mobile clock bias and enhances robustness.

2. Principle and Structure of the System

2.1. System Description

We consider a passive underwater localization system consisting of three fixed beacons with known positions $b_i \in R^3, i = 1,2,3$ and one mobile node with unknown position $\mathbf{p}(t)$ .Each beacon periodically transmits acoustic signals, and the mobile node only receives signals without transmitting. Due to independent local clocks, the beacons' transmission times include unknown offsets $\delta_i(t)$, which, if uncorrected, results in significant timing errors in time-of-arrival (TOA) measurements. The mobile node also has an unknown clock bias $\Delta(t)$. The propagation speed of sound is denoted by c , and measurement noise is present in all recorded times. Accurate localization thus requires compensating for both beacon clock offsets and the motion of the mobile node during signal propagation.

2.2. Overall Workflow

The localization procedure is executed in a round-by-round manner. In each measurement round, each beacon sequentially transmits a signal while other beacons and the mobile node record reception times. The inter-beacon reception times are first used to estimate and compensate the relative clock offsets among the fixed beacons. Once the beacons are synchronized, the mobile node's TOAs are corrected using these synchronized beacon times. Because the mobile node moves during signal propagation, TOAs are further adjusted via motion compensation, projecting them to a common reference position. Finally, differential TOA (dTOA) is computed, forming pairwise differences between motion-compensated TOAs to eliminate the unknown mobile node clock bias. The mobile node position is then estimated by solving the resulting nonlinear equations using least squares. This round-by-round approach ensures synchronization and motion compensation are applied in every cycle, maintaining high localization accuracy despite clock offsets, motion, and noise. A flowchart can be included to visualize the procedure.

2.3. Inter-Beacon Clock Synchronization

In practical systems, the clocks of fixed beacons are generally unsynchronized. To correct this, each beacon sequentially transmits a signal in each round, and other beacons record reception times. The measured reception time at beacon k for a transmission from beacon i is

$$r_k^{(i,r)} = s_i^{(r)} + \tau_{ik} + \delta_k^{(r)} - \delta_i^{(r)} + n_k^{(i,r)}, i \neq k \tag{1}$$

Where $s_i^{(r)}$ is the transmission time, $\tau_{ik} = \frac{\|b_i - b_k\|}{c}$ is the propagation delay, $\delta_i^{(r)}$ and $\delta_k^{(r)}$ are the beacon clock offsets, and $n_k^{(i,r)}$ is measurement noise.

For each round, collecting all inter-beacon measurements allows us to form a linear system

$$\mathbf{r} = \mathbf{H}\boldsymbol{\delta} + \mathbf{n} \tag{2}$$

where $\mathbf{r}$ contains measured reception times minus propagation delays, $\mathbf{H}$ encodes clock differences between beacons, and $\boldsymbol{\delta} = [\delta_2^{(r)}, \delta_3^{(r)}]^\top$ .The least squares solution is

$$\hat{\boldsymbol{\delta}}^{(\mathbf{r})} = (\mathbf{H}^\top\mathbf{H})^{-1}\mathbf{H}^\top\mathbf{r} \tag{3}$$

The corrected beacon transmission times are obtained as

$$s_i^{(r),corr} = s_i^{(r)} - \hat{\delta}_i^{(r)}, i = 1,2,3 \tag{4}$$

This synchronization is repeated in every measurement round to prevent error accumulation. By performing synchronization before mobile node localization, TOAs from different beacons are referenced to a common time frame, which is essential for accurate localization.

2.4. Motion compensation

When the mobile node moves, the raw TOAs corresponding to different beacon transmissions do not represent the same reception position or time. Put differently, the mobile node cannot be assumed stationary across the short but finite time intervals separating the arrivals from different beacons; this mismatch biases localization if not corrected. To mitigate this bias we propose a round-wise TOA adjustment to project all measurements to a unified reference time within each round.

Define the mobile node's recorded reception times $T_i^{(j)} \equiv r_{mob}^{(i,j)}$ and the raw TOA (after beacon-time correction) as

$$\tilde{\tau}_i^{(j)} = T_i^{(j)} - s_i^{(j),corr} \tag{5}$$

We construct a corrected TOA $\tau_i^{(j),corr}$ by using the relative timing between the current and previous rounds together with the earliest arrival in the current round. Specifically, let beacon 1 denote the earliest arrival in round j (i.e. $T_1^{(j)} = \min T_i^{(j)}$). Then we define

$$\tau_i^{(j),corr} = \tilde{\tau}_i^{(j)} - \frac{T_i^{(j)} - T_1^{(j)}}{T_i^{(j)} - T_i^{(j-1)}}(\tilde{\tau}_i^{(j)} - \tilde{\tau}_i^{(j-1)}) \tag{6}$$

This formulation can be interpreted as a first-order motion compensation derived under a near-linear motion assumption. Between consecutive cycles, the AUV displacement is small compared with the inter-beacon spacing, so its instantaneous position can be approximated by

$$\mathrm{p}(t) \approx \mathrm{p}(t_1^j) + \mathrm{v}(t_1^j)(t - t_1^j) \tag{7}$$

Substituting this linear motion model into the propagation-delay relation and retaining first-order terms yields equation (6), which effectively projects all measured delays to the common reference epoch t_1^j .

The numerator $T_i^{(j)} - T_m^{(j)}$ reflects the intra-cycle reception spacing among beacons, while the denominator $T_i^{(j)} - T_i^{(j-1)}$ describes the inter-cycle timing evolution caused by AUV motion. Under moderate inter-cycle intervals, equation (6) provides a consistent correction for displacement-induced delay bias and allows all beacon measurements to correspond to the same effective reception position.

2.5. TOA equations and differential formulation

After motion compensation, the TOA associated with beacon i in round j is modeled by the standard geometric relation augmented by the mobile clock bias:

$$\tau_i^{(j),corr} = \frac{\| \mathbf{p}_j - \mathbf{b}_i \|}{c} + \Delta^{(j)} + \varepsilon_i^{(j)}, i = 1,2,3 \tag{8}$$

where $\Delta^{(j)}$ denotes the mobile node's unknown clock bias in round j and $\varepsilon_i^{(j)}$ collects residual errors (measurement noise, residual synchronization error, and model mismatch).

To eliminate $\Delta^{(j)}$, we take pairwise differences of (7). For completeness we write the three pairwise dTOAs in round j

$$d_{21}^{(j)} = \tau_2^{(j),corr} - \tau_1^{(j),corr} = \frac{\| \mathrm{p}_j - \mathrm{b}_2 \| - \| \mathrm{p}_j - \mathrm{b}_1 \|}{c} + \eta_{21}^{(j)} \tag{9}$$

$$d_{31}^{(j)} = \tau_3^{(j),corr} - \tau_1^{(j),corr} = \frac{\| \mathrm{p}_j - \mathrm{b}_3 \| - \| \mathrm{p}_j - \mathrm{b}_1 \|}{c} + \eta_{31}^{(j)} \tag{10}$$

$$d_{32}^{(j)} = \tau_3^{(j),corr} - \tau_2^{(j),corr} = \frac{\| \mathrm{p}_j - \mathrm{b}_3 \| - \| \mathrm{p}_j - \mathrm{b}_2 \|}{c} + \eta_{32}^{(j)} \tag{11}$$

Where $\eta_{ik}^{(j)} = \varepsilon_i^{(j)} - \varepsilon_k^{(j)}$. Any two of the above equations (for example $d_{21}^{(j)}$ and $d_{31}^{(j)}$) are sufficient to determine p_j in two dimensions; the third serves as an independent verification. The position estimate is obtained by solving the nonlinear least-squares problem

$$\hat{p}_j = arg \min_{\mathrm{p}} \sum_{(i,k)\in S} \left[d_{ik}^{(j)} - \frac{\| \mathrm{p} - \mathrm{b}_i \| - \| \mathrm{p} - \mathrm{b}_k \|}{c} \right]^2 \tag{12}$$

Where S denotes the set of chosen independent pairs (e.g. $\{(2,1),(3,1)\}$). The minimization can be performed with a Gauss–Newton iteration or other standard nonlinear solvers; initial guess can come from previous round's position or from geometric intersection.

3. Simulation and Analysis

3.1. Simulation Setup

To evaluate the positioning performance under clock asynchronization and motion-induced errors, simulations were conducted with three fixed anchors and one mobile node. The anchors are placed at coordinates [0,0] m, [1000,0] m, [1000,1000] m. The mobile node moves along a predefined 2D trajectory, and its true positions are recorded for performance evaluation.

Each anchor sequentially emits positioning signals, and both anchors and the mobile node record reception times. The fixed nodes are first synchronized to a reference node using multiple rounds of two-way measurements. The TOA measured at the mobile node is affected by an unknown constant clock offset Δ as well as Gaussian measurement noise.

3.2. Positioning Methods

Four positioning schemes were implemented to investigate the effects of anchor synchronization and motion compensation:

- Method A: TOA without anchor synchronization or motion compensation
  This baseline assumes that the anchors and the mobile node are not synchronized, and no motion compensation is applied. The TOA measurements include both fixed-node and mobile-node clock offsets, leading to the largest positioning errors.

Journal of Physics: Conference Series **3178** (2026) 012054 doi:10.1088/1742-6596/3178/1/012054

- Method B: TOA with anchor synchronization
  The fixed nodes are first synchronized to a reference anchor. The TOA at the mobile node still contains its own unknown clock offset, but the elimination of fixed-node asynchronization reduces part of the error.
- Method C: TOA with anchor synchronization and motion compensation
  In addition to anchor synchronization, motion compensation is applied. Each TOA measurement is adjusted according to the mobile node's movement between signal receptions, accounting for the fact that the mobile node does not receive all signals at the same location or time.
- Method D: dTOA with anchor synchronization and motion compensation
  Differential TOA is applied to the motion-compensated signals. By taking differences between TOAs with respect to a reference anchor, the unknown mobile-node clock offset Δ is effectively eliminated, yielding the most accurate positioning results.

3.3. Simulation Parameters
The main simulation parameters are summarized in Table 1.

Table 1. Simulation Parameters.

Parameter	Value	Description
Number of anchors	3	Fixed nodes
Mobile node trajectory	Predefined 2D path	True positions recorded for evaluation
Sound speed c	1500 m/s	Constant
Mobile node clock offset Δ	10μs	Constant
Measurement noise σ	100 ns	Gaussian distributed
Simulation rounds	20	Each anchor transmits once per round

The simulation follows this procedure for each round:

- Anchor transmission and synchronization: All anchors sequentially transmit, and the other anchors record reception times to synchronize with the reference node.
- Mobile node reception: The mobile node records TOA for each transmitted signal.
- Motion compensation (Methods C & D): The TOA measurements are corrected according to the mobile node's motion between receptions.
- Position estimation: TOA or dTOA methods are applied according to the selected scheme (A–D).
- Error computation: The estimated position is compared with the true mobile node position, and the RRMSE is calculated over all rounds.

3.4. Simulation Results and Analysis
Figure 1 shows the estimated trajectories of the mobile node for all four methods. Method A (no synchronization, no compensation) exhibits significant deviation from the true trajectory due to combined fixed-node and mobile-node clock offsets. Method B (synchronized anchors) reduces part of the bias but still suffers from mobile-node clock offset. Method C (synchronization + motion compensation) further improves accuracy by accounting for the mobile node's movement. Method D (synchronization + motion compensation + dTOA) achieves the highest accuracy, effectively removing the mobile-node clock bias.

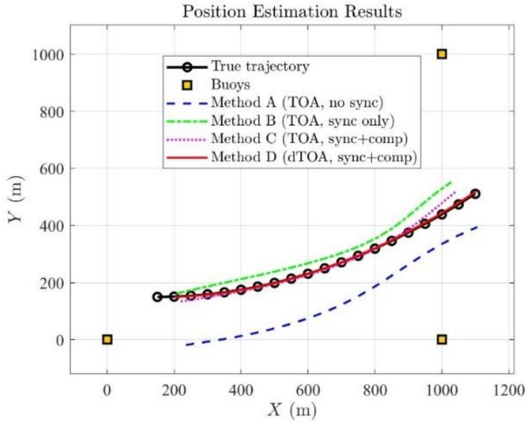

Figure 1. Position estimation results of the mobile node under four methods (A–D).

To quantitatively evaluate the localization performance, the position error was calculated for each localization round as the Euclidean distance between the estimated and true positions. The per-round errors are shown in Figure 2. It can be seen that Method A produces the largest and most fluctuating errors, often exceeding several meters due to asynchronous time bases. Method B reduces the error magnitude but still shows instability over time. Method C provides a substantial improvement in both accuracy and consistency, while Method D maintains the lowest and most stable error curve throughout all localization rounds. Overall, the per-round error trend further confirms the progressive improvement from A to D, and demonstrates that synchronization, motion compensation, and differential processing jointly contribute to enhanced positioning stability and precision.

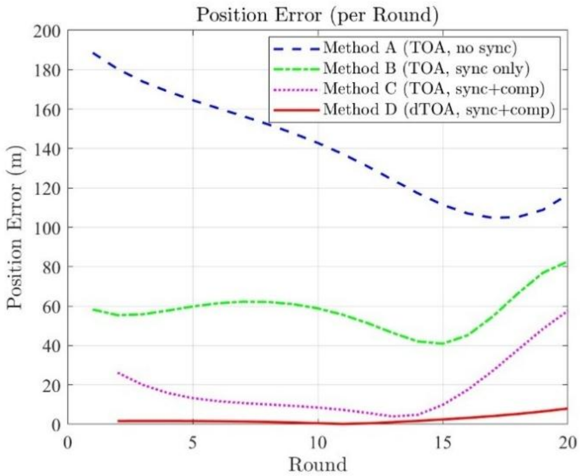

Figure 2. Position error per localization round for four methods (A–D).

The Relative Root-Mean-Square Error (RRRMSE) was computed over all localization points as:

$$RRMSE = \frac{1}{D_{\max}} \sqrt{\frac{1}{N} \sum_{k=1}^{N} \left\| \hat{\mathbf{p}}_{\mathbf{k}} - \mathbf{p}_{\mathbf{k}}^{\mathbf{true}} \right\|^2} \tag{13}$$

Where $\hat{\mathbf{p}}_{\mathbf{k}}$ and $\mathbf{p}_{\mathbf{k}}^{\mathbf{true}}$ denote the estimated and ground-truth AUV positions at the k -th measurement, and $D_{\max}$ represents the maximum inter-node distance among all anchors.

The RRMSE for each method is summarized in Table 2. Method A has the largest error, followed by Method B, Method C, and finally Method D with the smallest RRMSE. Overall, Method D achieves an average RRMSE reduction of 89.5% compared with the unsynchronized baseline.

This demonstrates that anchor synchronization, motion compensation, and differential processing each contribute to improved localization accuracy, with dTOA providing the most robust solution against mobile-node clock asynchronization. This indicates that the proposed method effectively mitigates both synchronization and motion-induced errors, providing a stable localization performance even under asynchronous conditions.

Table 2. RRMSE comparison of four methods.

Method	RRMSE	Description
A	0.101	No synchronization, no motion compensation
B	0.041	Synchronized anchors, no motion compensation
C	0.019	Synchronized anchors with motion compensation
D	0.011	Synchronized anchors with motion compensation + dTOA

4. Sea Trial Analysis

4.1. Experimental Setup and Procedure

To verify the practical effectiveness of the proposed synchronization and motion-compensation framework, a sea trial was conducted in the South China Sea. The experimental system consisted of three fixed acoustic beacons and one autonomous underwater vehicle (AUV) acting as a passive receiving node. The fixed beacons were moored at known positions and equipped with underwater acoustic modems, while the AUV carried a hydrophone for signal reception.

At the beginning of each localization cycle, the three beacons sequentially transmitted acoustic pulses, and the other beacons recorded the corresponding reception times. Based on these inter-beacon measurements, mutual synchronization was performed so that all beacon clocks were aligned to a common time reference (anchor A). After synchronization, the AUV received the signals from all three synchronized beacons during its motion.

Each localization cycle consisted of three transmissions (one from each beacon). A total of 14 localization cycles were completed while the AUV followed a predefined trajectory. The trajectory was reconstructed from the AUV's navigation log (heading and speed data) and used as the ground-truth reference for performance evaluation.

4.2. Experimental Results and Discussion

Figure 3 shows the estimated AUV trajectories for Methods A–D, compared with the reconstructed ground-truth trajectory derived from the navigation log.

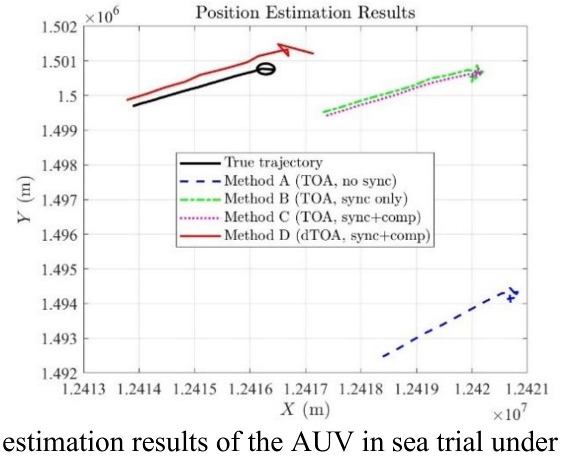

Figure 3. Position estimation results of the AUV in sea trial under four methods (A–D).

Method A (unsynchronized TOA) exhibits significant deviation, especially in the later stages, due to accumulated clock drift between nodes. Method B (synchronized TOA) shows improvement, reducing the constant bias component caused by inter-node offset. Method C (synchronized + compensated TOA) further improves accuracy, demonstrating the benefit of correcting for AUV movement during signal reception. Method D (synchronized + compensated dTOA) produces a trajectory that closely matches the ground-truth, indicating that differential TOA effectively eliminates the remaining time offset between the fixed nodes and the mobile AUV.

Figure 4 presents the positioning errors per round for all four methods. It can be seen that the error variance significantly decreases after synchronization and motion compensation, while the dTOA-based approach provides the most stable performance across all test intervals.

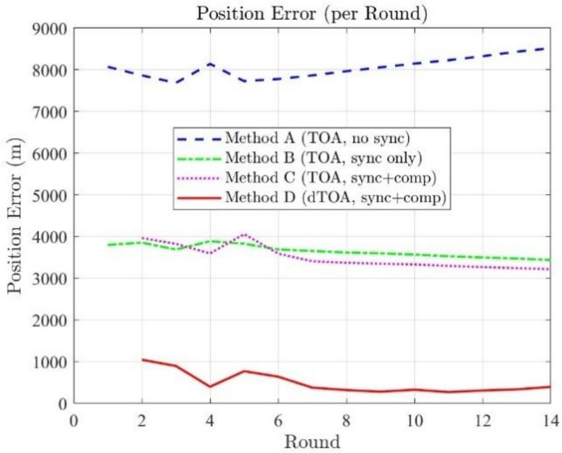

Figure 4. Positioning error per round under four methods (A–D) in sea trial.

Table 3 summarizes the average RRMSE values for all methods. Compared with the baseline (Method A), the proposed synchronization and motion-compensated dTOA method (Method D) reduces the average error by over 93%, confirming its robustness under real oceanic conditions with measurement noise and environmental uncertainty.

Table 3. RRMSE comparison of different methods based on sea trial data.

Method	RRMSE	Description
A	0.366	No synchronization, no motion compensation
B	0.166	Synchronized anchors, no motion compensation
C	0.160	Synchronized anchors with motion compensation
D	0.025	Synchronized anchors with motion compensation + dTOA

5. Conclusions

This paper investigated a synchronization-compensated underwater acoustic localization method based on the TOA principle, aiming to improve positioning accuracy for moving AUVs under asynchronous and dynamic ocean conditions. A complete framework was established, including inter-node clock synchronization, motion compensation for mobile platforms, and a refined differential TOA estimation scheme.

Simulation results demonstrated that, compared with traditional TOA localization without synchronization, the proposed method effectively reduces systematic errors caused by clock offsets and motion-induced timing deviations. Among the four tested methods, the combination of synchronization, motion compensation, and dTOA yielded the lowest RRMSE and the most stable trajectory estimation performance. These results confirm that the proposed method can effectively mitigate timing bias and environmental uncertainty, offering practical value for high-precision AUV localization in complex marine environments.

Although the proposed method effectively addresses time asynchrony and motion-induced errors in underwater localization, it assumes a horizontally homogeneous and temporally stable sound speed during both simulation and sea trials. In practical ocean environments, however, spatial and temporal variations in the sound-speed field can introduce additional range biases. Future work will extend the current framework by incorporating profile-adaptive or ray-based sound-speed correction models to further enhance positioning accuracy under complex ocean conditions.

6. References

[1] Toky A, Singh R P and Das S 2020 Localization schemes for Underwater Acoustic Sensor Networks - A Review *Computer Science Review* **37** 100241
[2] Luo J, Yang Y, Wang Z and Chen Y 2021 Localization Algorithm for Underwater Sensor Network: A Review *IEEE Internet of Things Journal* **8** 13126–44
[3] Diamant R and Lampe L 2013 Underwater Localization with Time-Synchronization and Propagation Speed Uncertainties *IEEE Transactions on Mobile Computing* **12** 1257–69
[4] Cario G, Casavola A, Gagliardi G, Lupia M and Severino U 2021 Accurate Localization in Acoustic Underwater Localization Systems *Sensors* **21** 762
[5] Chaudhary M, Goyal N, Benslimane A, Awasthi L K, Alwadain A and Singh A 2023 Underwater Wireless Sensor Networks: Enabling Technologies for Node Deployment and Data Collection Challenges *IEEE Internet of Things Journal* **10** 3500–24
[6] Han G, Zhang C, Shu L and Rodrigues J J P C 2015 Impacts of Deployment Strategies on Localization Performance in Underwater Acoustic Sensor Networks *IEEE Transactions on Industrial Electronics* **62** 1725–33
[7] Yang Y and Qin X 2021 Resilient observation models for seafloor geodetic positioning *J Geod* **95** 79
[8] Liu M, Liu J, Wang G, Pan X, Peng Z and Cui J-H 2024 LITM: Localization With Insufficient TOA Measurements for Unsynchronized Mobile Nodes in Underwater Acoustic Networks *IEEE Internet of Things Journal* **11** 33642–56
[9] Gong Z, Li C, Jiang F and Zheng J 2020 AUV-Aided Localization of Underwater Acoustic Devices Based on Doppler Shift Measurements *IEEE Transactions on Wireless Communications* **19** 2226–39
[10] Yao X, Zhangming H, Jiongqi W, Xuanying Z, Yuyun C and Xiaogang P 2023 TOA positioning algorithm of LBL system for underwater target based on PSO *Journal of Systems Engineering and Electronics* **34** 1319–32
[11] Gola K K 2024 A comprehensive survey of localization schemes and routing protocols with fault tolerant mechanism in UWSN- Recent progress and future prospects *Multimed Tools Appl* **83** 76449–503
[12] Shams R, Otero P, Aamir M and Khan F H 2021 Joint Algorithm for Multi-Hop Localization and Time Synchronization in Underwater Sensors Networks Using Single Anchor *IEEE Access* **9** 27945–58
[13] Xing Y, Wang J, He Z, Chen Y and Zhou X 2024 An identification method of LBL underwater positioning systematic error with optimal selection criterion *Sci Rep* **14** 21432
[14] Chen G, Liu Y, Liu Y, Tian Z and Li M 2019 Adjustment of Transceiver Lever Arm Offset and Sound Speed Bias for GNSS-Acoustic Positioning *Remote Sensing* **11** 1606
[15] Yu M, Geng H and Liu X 2025 Underwater vehicle positioning method using sound speed error estimation in conjunction with a motion compensation model *Ocean Engineering* **319** 120241
[16] Jin Z, Ding M, Luo Y and Li S 2019 Integrated Time Synchronization and Multiple Access Protocol for Underwater Acoustic Sensor Networks *IEEE Access* **7** 101844–54
[17] Ouyang Y, Han Y, Wang Z and He Y 2024 Underwater Network Time Synchronization Method Based on Probabilistic Graphical Models *Journal of Marine Science and Engineering* **12** 2079

Acknowledgments
This work was supported by the Fundamental Research Funds for the Central Universities (No. 2242025F20003).